



## Spin polarization in photoelectron spectroscopy from antiferromagnets: Cr films on Fe(1 1 0) from first principles

P. Bose<sup>a</sup>, P. Zahn<sup>a</sup>, I. Mertig<sup>a,b</sup>, J. Henk<sup>b,\*</sup>

<sup>a</sup> Martin-Luther-Universität Halle-Wittenberg, Institut für Physik, D-06099 Halle (Saale), Germany

<sup>b</sup> Max-Planck-Institut für Mikrostrukturphysik, Weinberg 2, D-06120 Halle (Saale), Germany

### ARTICLE INFO

#### Article history:

Received 24 February 2010

Accepted 17 August 2010

Available online 24 August 2010

#### PACS:

79.60.Dp

73.20.At

72.25.+z

75.50.Ee

#### Keywords:

Photoelectron spectroscopy

Antiferromagnets

Spin polarization

Chromium

Iron

First-principles calculations

### ABSTRACT

The spin- and angle-resolved photoelectron spectroscopy from ultrathin Cr films on Fe(110) is investigated by means of first-principles electronic structure and photoemission calculations. The antiferromagnetic ordering in the Cr films leads in dependence on film thickness to a rapidly decreasing and oscillating photoelectron spin polarization, in reasonable agreement with recent experiments (Dedkov (2007) [1]). The oscillation period is explained by quantum-well states in the Cr film and by a Fermi surface nesting vector. The importance of transition matrix elements is highlighted. The findings point to a noncollinear magnetic structure at the Fe/Cr interface.

© 2010 Elsevier B.V. All rights reserved.

### 1. Introduction

The electronic and magnetic structure of ultrathin films shows a variety of effects, depending on the substrate material, the crystal orientation, the film thickness, and other characteristic quantities. The situation becomes even more demanding for detailed investigations if antiferromagnetic (AFM) materials – like Mn or Cr – are grown on a ferromagnetic (FM) substrate – like Fe. One of the prominent effects is exchange bias (e.g. [2–7]). It appears if the magnetic moments of both the ferromagnet and the antiferromagnet are aligned parallel, leading to uncompensated moments in the antiferromagnet.

Further, the magnetic order at the ferromagnet/antiferromagnet interface can be frustrated (for frustration at step edges see Ref. [8]). In such a case, the magnetic structure at the interface can differ considerably from that of the respective bulk systems. This competition between the antiferromagnetic couplings (AFM–AFM and AFM–FM) leads in particular to noncollinear magnetic configurations, in order to form or at least to arrive at almost compensated spin structures [9–13].

Instead of forming noncollinear structures, the frustration at the FM/AFM interface can also be reduced by a layer-wise AFM configuration, as shows up in Mn films on Fe(001) or in Cr interlayers in Fe(001)/Cr/MgO/Fe(001) magnetic tunnel junctions [14,15]. Another solution would be to reduce the magnetic moments. This could be realized by the formation of an incommensurate spin density wave (SDW) which was found in bulk Cr. For thin Cr films this magnetic order is suppressed and the commensurate SDW with 2 monolayer (ML) oscillation period forms the layer-wise AFM order [16].

As it is evident from the preceding, Cr and Fe show a variety of magnetic structures (for a review of the rich magnetic structure of Cr, see Ref. [17]). Especially Cr films on Fe(001) were subject to a considerable number of experimental and theoretical investigations, applying a variety of methods (without any claim of completeness, we refer to Refs. [18–24]). In contrast, ultrathin Cr films on Fe(110) are comparably less investigated and, consequently, less understood. Among other advanced spin-dependent spectroscopies, like spin-resolved scanning tunneling microscopy [25–27] and spin-polarized low-energy electron diffraction [28,29], spin- and angle-resolved photoemission is a powerful method to investigate the electronic and magnetic structure of surfaces and ultrathin films [30–32], also of noncollinear magnetic configurations [33,34].

\* Corresponding author.

E-mail address: [henk@mpi-halle.de](mailto:henk@mpi-halle.de) (J. Henk).

Recent spin-resolved photoemission experiments by Dedkov [1] show that the spin polarization of photoelectrons which are excited from the Fermi energy decreases rapidly with increasing Cr film thickness and oscillates with a period of about 2 ML. The decrease can be attributed to a decreasing net magnetization as probed by the photoelectrons. The decay rate would be determined by the photoelectron escape depth, typically of the order of a few monolayers [35–37], or the screening of the distortion of the AFM order at the interface, which appears on a similar length scale. This finding provides evidence for an antiferromagnetic order in the Cr film, in particular at the surface of thicker Cr films.

The oscillation with film thickness can on one hand be attributed to a layer-wise antiferromagnetic (LAFM) order which explains the 2 ML period in a natural way. Note that layer-wise antiferromagnetic order was observed in Mn films on Fe(001), especially in films thicker than about 6 ML [14,38,39]. However, a recent first-principles investigation on Cr(110)/Fe(110) [40] does not support LAFM order. On the contrary, a magnetic structure which is compatible with the AF<sub>0</sub> magnetic structure of bulk Cr, with increased local magnetic moments at the Cr(110) surface, is found.

On the other hand, it is speculated in Ref. [1] that the oscillation may be due to spin-polarized quantum-well states in the Cr film, as is observed in (001)-oriented Cr films [41]. Then the question arises how the period can be explained by the band-structure of bulk Cr. (Quantum-size effects in photoemission are discussed in Ref. [42]).

Further, one has to be cautious to explain the photoelectron spin polarization in terms of local magnetic moments. Being a ground-state property, the latter are computed from the spin-resolved density of states (DOS) for a specified site ('atom') and involve integration over all energies up to the Fermi level and integration over all in-plane wavevectors  $k_{\parallel}$ . In contrast, the spin-dependent photocurrent, as an excited-state property, is obtained for a single wavevector (in angle-resolved photoemission) and is strongly determined by transition matrix elements, dipole selection rules, and the inelastic mean free path [43,44]. This implies that a direct comparison, even with the spectral density (that is the energy- and wavevector-resolved local DOS), may be misleading. In turn, these imponderabilities call for theoretical photoemission intensities which provide a direct link between ground-state properties, as obtained by density functional theory, and experimental spectra.

While the theoretical investigation of Johnson et al. [40] focused on the electronic and magnetic properties of the Fe–Cr interface, and thus addresses Cr films 6–10 ML thick, a detailed study of Cr films in the experimental thickness range of 0–6 ML is missing.

In this paper we report on a theoretical investigation of the spin- and angle-resolved photoemission from Cr films on Fe(110), with a focus on the dependence of the photoelectron spin polarization on Cr film thickness. The photoemission calculations relate experimental data, as reported especially in Ref. [1], with ground-state properties which are obtained by *ab initio* electronic-structure calculations. Since a number of free parameters enter the photoemission calculations perfect agreement of theory with experiment cannot be expected [43]. Hence, we focus in this work on trends, not on details.

The paper is outlined as follows. Theoretical aspects are addressed in Section 2. The results are presented and discussed in Section 3. Concluding remarks and an outlook are given in Section 4.

## 2. Theoretical

The electronic and magnetic structure calculations were performed within the local spin-density approximation to density functional theory in the parameterization of Vosko et al. [45].

The computations rely on multiple-scattering theory as formulated in the Korringa–Kohn–Rostoker (KKR) method [46–48]. The first-principles calculations were performed for uncovered Fe(110) and Cr films on Fe(110) with thicknesses ranging from 1 to 6 ML, named Cr<sub>x</sub>/Fe(110) with  $x=0, \dots, 6$  in the following.

Bulk Cr crystallizes in the body-centered cubic (bcc) structure with AF<sub>0</sub> antiferromagnetic order. Sites in the corners of the bcc cube have magnetic moments  $+\vec{M}$ , center sites have  $-\vec{M}$  [49,50], with  $\vec{M}$  oriented along a cube edge. If this bulk magnetic structure is continued at the Cr(110) surface, each two-dimensional (2D) unit cell contains two oppositely magnetized sites, named sites 1 and 2 in the following. The shape anisotropy typically forces in-plane orientation [51–54]. Hence, we assume the local moments to be in-plane and oriented along the easy axis of Fe(110) (i.e. the  $[\bar{1}10]$  direction). We note in passing that a neutron diffraction study on (110)-oriented Fe/Cr multilayers found Cr moments along  $[100]$  or  $[010]$ , i.e. perpendicular to the Fe moments (along  $[001]$ ) [49,50].

As a consequence of the AFM order in the Cr films, each 2D unit cell in the Fe substrate has to contain also two sites. Since neighboring Fe atoms couple ferromagnetically and neighboring Cr atoms couple antiferromagnetically, there is magnetic frustration at the Fe–Cr interface. Therefore, one might expect noncollinear magnetism or a reduction of the magnetic moments at the Fe–Cr interface. It is expected to evolve towards an AF<sub>0</sub> or LAFM order at the films' surface, in particular for the thicker Cr films.

Another important issue in surface physics is the geometric relaxation at surfaces and interfaces. For uncovered Fe(110), an inward relaxation of the outermost surface layer (S) by  $-0.5\%$  of the interlayer distance of bulk Fe is obtained by low-energy electron diffraction analysis [56]. For the Cr-covered Fe surface we adopt the theoretical findings of Johnson et al. [40]: the interlayer distance in the interior of the Cr films is  $+1\%$  with respect to the Fe–bulk spacing. At the Fe–Cr interface, the interlayer spacing is reduced by  $-1\%$  and at the Cr surface by  $\pm 0\%$ , as is obtained by first-principles calculations for Cr films of up to 10 ML thickness. The buckling within the Cr layers, that is different  $z$  positions of oppositely magnetized sites, is neglected, in agreement with the findings of Ref. [40]. We note in passing that photoemission spectra for the unrelaxed structure do not differ significantly from those for the relaxed structure. Thus, relaxation is of minor importance for the issues addressed in this work.

Spin-resolved photoemission intensities are obtained within the relativistic one-step model [57], as formulated in layer-KKR. The latter is implemented in the OMNI program package for electron spectroscopies [58] which has proven its reliability in a series of publications (see, e.g. Ref. [59]). Convergence with respect to free parameters was checked. For example, the maximum angular momentum is  $l_{\max}=4$  and the number of plane waves used in the interlayer scattering is larger than 100. The number of surface layers which contribute to the photocurrent exceeds 30. Note that it is accounted for the correct boundary conditions, that is, Cr films supported by a semi-infinite Fe substrate.

Correlation effects are described by an energy-dependent self-energy  $\Sigma(E)$ . Its imaginary part increases quadratically at the Fermi energy  $E_F$  and saturates with increasing energetic distance from  $E_F$ . Its real part shifts occupied states closer to  $E_F$ , thereby reduces the band width and the exchange splitting. Instead of modeling real and imaginary part differently by power laws, as in Ref. [60], we adopted a model self-energy which parameterizes simultaneously real and imaginary part of  $\Sigma(E)$  and shows the correct behaviour at  $E_F$  as well as the correct asymptotics for very large and very small energies [61]. The parameters were obtained by fitting theoretical photoemission intensities of Fe(110) to those reported in Refs. [1,60]. The Fe self-energy was also assumed for the Cr films.

The photoemission set-up is chosen as described in Ref. [1]. The in-plane magnetization is along the  $[\bar{1}10]$  direction. The photoelec-

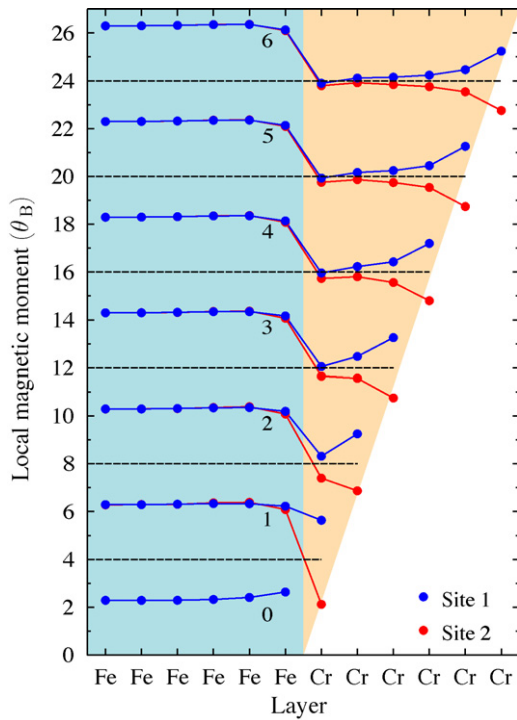


**Fig. 1.** Atom-resolved magnetic profiles of  $\text{Cr}_x/\text{Fe}(1\ 1\ 0)$ , with Cr film thickness  $x = 0, \dots, 6$  ML. Data for sites 1 and 2 are given in blue and red, respectively. The spectra are offset by  $4\ \mu_B$  for clarity, with respective zeroes indicated by dashed lines. The film thickness  $x$  is indicated as well. The Fe (Cr) region is further emphasized by a blue (tan) background. (For interpretation of the references to color in this figure legend, the reader is referred to the web version of the article.)

trons are detected in normal emission ( $\vec{k}_{\parallel} = \vec{0}$ ). Due to symmetry, the spin polarization is normal to the scattering plane which is spanned by the surface normal and the incidence direction of the light. The latter impinges within the  $(\bar{1}\ 1\ 0)$  plane, that is perpendicular to the magnetization, with a polar angle of  $30^\circ$  with respect to the surface normal. The unpolarized light with 21.2 eV photon energy ( $\text{He}_I$ ) is mimicked by incoherent superposition of s- and p-polarized radiation.

The above set-up is the standard set-up for magnetic linear dichroism (MLD) [60,62–64]. Computations for reversed magnetization ( $-\vec{M}$ ), however, show that the asymmetry of the two photocurrents  $I(+\vec{M})$  and  $I(-\vec{M})$  is negligibly small for Cr-covered  $\text{Fe}(1\ 1\ 0)$ . Consequently, MLD is not considered in this work.

### 3. Results and discussion

#### 3.1. Magnetic structure

The magnetic structure of  $\text{Cr}/\text{Fe}(1\ 1\ 0)$  is discussed in terms of magnetic profiles, that are site-resolved local magnetic moments. Since there are two sites per 2D unit cell (except for uncovered  $\text{Fe}(1\ 1\ 0)$ ), there are two profiles, one for site 1, the other for site 2.

The uncovered Fe surface shows an increased magnetic moment at the surface (bottom curves in Fig. 1), as was deduced by Tamura and coworkers [65] (for  $\text{Fe}(0\ 0\ 1)$  see for example [66]). The moment of the outermost surface layer is increased by 15% with respect to the bulk value ( $2.63\ \mu_B$  versus  $2.29\ \mu_B$ ).

The system  $\text{Cr}_1/\text{Fe}(1\ 1\ 0)$  displays an uncompensated magnetic configuration, with magnetic Cr moments of  $1.64\ \mu_B$  (site 1) and  $-1.88\ \mu_B$  (site 2). The Fe moments at the interface are slightly reduced with respect to the bulk value ( $2.23\ \mu_B$  for site 1 and  $2.09\ \mu_B$  for site 2).

Already for  $\text{Cr}_2/\text{Fe}(1\ 1\ 0)$  the tendency to overcome the magnetic frustration at the interface by reduction of the Cr moments becomes evident. It is clearly seen for  $\text{Cr}_6/\text{Fe}(1\ 1\ 0)$  for which the interface Cr moments are as small as  $-0.10\ \mu_B$  (site 1) and  $-0.21\ \mu_B$  (site 2).

The reduction becomes less when approaching the surface. Here, the  $\text{AF}_0$  structure of bulk Cr is established but with layer-dependent moments. For example,  $\text{Cr}_6/\text{Fe}(1\ 1\ 0)$  has moments of  $\pm 1.24\ \mu_B$  in the surface layer. Due to the smaller lattice constant of Fe we find a moment in bulk-like Cr films of  $0.6\ \mu_B$  (in bulk Cr moment is  $1.09\ \mu_B$ , from Ref. [40]).

In summary, we find similar profiles as reported in Ref. [40] but with stronger reductions at the Fe–Cr interface. A layer-wise AFM configuration is clearly ruled out. But due to the applied computational method, we cannot exclude a noncollinear magnetic structure.

#### 3.2. Spin-resolved photoemission

Already the above findings support qualitatively a decrease of the photoelectron spin polarization with increasing Cr film thickness. Due to the finite escape depth  $\lambda$  (surface sensitivity), the photoelectrons probe an effective net magnetic moment which can be mimicked by summing up all local magnetic moments but weighted by the attenuation factor  $\exp(-nd/\lambda)$  (with  $n$  layer number and  $d$  interlayer distance). This results in a strong decay of the (positive) effective moment which can be very well described by an exponential. However, within this very simple model neither the oscillations nor the sign of the observed photoelectron spin polarization (ESP) can be explained. Regarding the latter, note that the ESP at the Fermi energy is negative for both  $\text{Fe}(1\ 1\ 0)$  and  $\text{Fe}(0\ 0\ 1)$ , in contrast to the net moment.

Theoretical photoemission intensities for the set-up described in Section 2 are displayed in Fig. 2. The spin-averaged spectrum of  $\text{Fe}(1\ 1\ 0)$  (bottom in Fig. 2) compares well with that reported in Ref. [60]. We find also agreement with the spin-resolved data from Dedkov [1], especially in the size of the spin polarization at large binding energies (about 60%). Note the spin polarization of the high-binding energy tails decreases rapidly with Cr film thickness, in agreement with the above model and the experiment [1].

While the spectra show no distinct structures at energies less than, say,  $-0.75$  eV, dispersive maxima and shoulders appear in particular in the energy range from  $-0.45$  eV up to the Fermi energy. Note that these structures are hardly visible in the spin-averaged data but clearly show up in the spin-resolved intensities, a clear benefit of the spin resolution.

The photoelectron spin polarization at the Fermi energy decreases strongly with increasing Cr film thickness (see Fig. 3). The dispersion of spin-polarized QWS (Fig. 2) leads to an oscillation, thereby supporting the speculation by Dedkov [1]. To determine the oscillation period we performed two fits in succession. The first fit accounts for the exponential decay of the ESP  $P$ ,  $P_1(x) = a \exp(-x/b) + c$  with  $x$  being the film thickness in ML. We find  $a = -98\%$ ,  $b = 2.47$  ML and  $c = 7\%$ , in reasonable agreement with the  $\text{AF}_0$  magnetic structure. Note that spin-orbit coupling can result in a finite spin polarization even from nonmagnetic surfaces [67]. Hence, the nonzero value of  $c$  could be attributed to spin-orbit coupling.

The second fit accounts for the oscillatory component of the ESP,  $P_2(x) = P_1(x) + d \cos(x/e) + f$ . The period  $e$  is estimated to 2.8 ML, a number which hardly agrees with that in experiment ( $\approx 2$  ML [1]). This inconsistency may be explained by a noncollinear magnetic structure at the Fe–Cr interface which, however, requires further experimental and theoretical investigations.

To explain the theoretical oscillation period, a very careful analysis in terms of the Cr bulk band-structure is performed. As shown in Fig. 1, the magnetic moments of the inner Cr layers are strongly

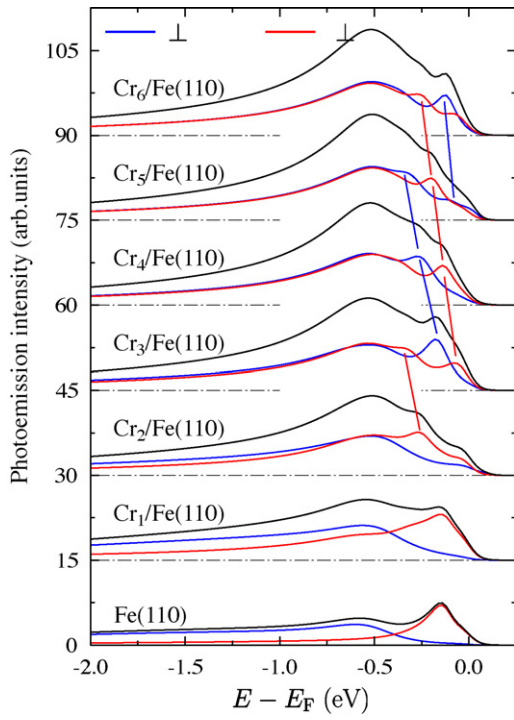


**Fig. 2.** Theoretical spin-resolved photoemission from  $\text{Cr}_x/\text{Fe}(110)$ , with Cr film thickness  $x = 0, \dots, 6$  ML (as indicated on the l.h.s. of each spectrum). The normal-emission spectra are vertically offset for clarity, with the respective zeroes indicated by dashed-dotted lines. Blue for spin-up, red for spin-down, and black solid lines for spin-averaged intensities. The dispersion of maxima which are associated with spin-polarized quantum-well states is emphasized by color-coded lines which serve as guide to the eye. For details of the set-up, see Section 2. (For interpretation of the references to color in this figure legend, the reader is referred to the web version of the article.)

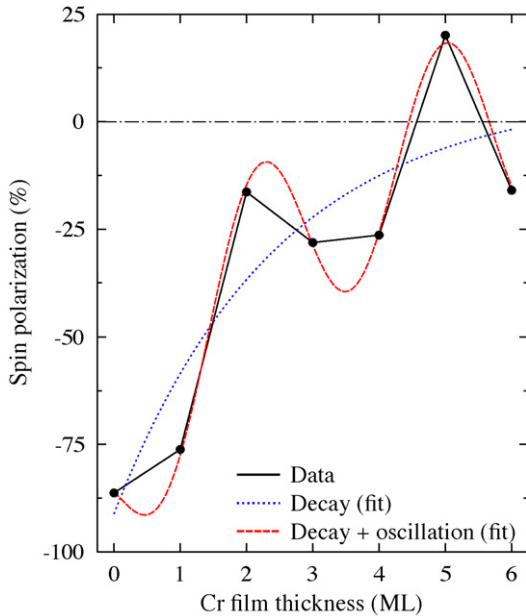


**Fig. 3.** Photoelectron spin polarization at the Fermi energy  $E_F$  versus Cr film thickness (filled circles, black solid line), as obtained from the spectra shown in Fig. 2. The blue dotted line represents an exponential decay,  $a \exp(-bx) + c$ , fitted to the data. The red dashed line includes in addition an oscillatory component,  $d \cos(x/e + f)$ , also fitted to the data. (For interpretation of the references to color in this figure legend, the reader is referred to the web version of the article.)

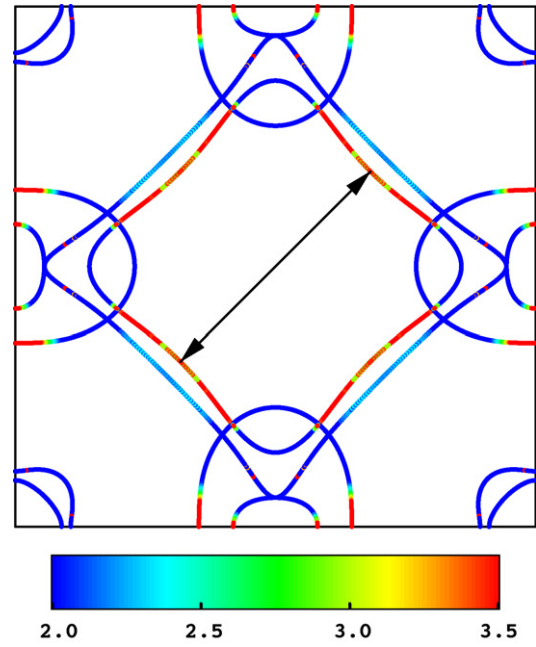


**Fig. 4.** Section of the Fermi surface of bcc Cr with antiferromagnetic  $\text{AF}_0$  order in the  $(001)$  plane inside the first Brillouin zone of the CsCl structure. The nesting vector along the  $[110]$  direction which corresponds to an oscillation period of 2.75 ML is indicated. The color code gives the effective mass (in units of the electron mass) in the directions perpendicular to the Fermi surface normal.

suppressed, but they recover for larger thicknesses. Assuming a bulk-like electronic structure in the interior Cr layers, the oscillatory response is determined by the Fermi surface nesting vector in the  $(110)$  direction at the considered  $k_{\parallel}$ . The corresponding section of the Fermi surface for LAFM Cr in the CsCl structure is given in Fig. 4. The arrow marks the nesting vector which connects stationary points with the largest contribution to the susceptibility, which is determined by a large effective mass. The color code of the section line gives the effective mass

$$m^* = \sqrt{\frac{d^2 E}{dk_1^2} \frac{d^2 E}{dk_2^2}}^{-1} \quad (1)$$

in the directions perpendicular to the Fermi surface normal. The period obtained from the L-AFM structure is 2.75 ML. It changes slightly to 2.88 ML when considering a PM state with zero magnetic moments at the Cr sites. In the PM configuration, all states are spin-degenerate in the bulk.

The occurrence of spin-polarized quantum-well states found here points to the importance of the spin-dependent reflection at the Fe–Cr interface. The sensitivity of the quantum wells on the spin-dependent reflection at the Fe–Cr interface is proven by deliberately altering the magnetic structure of the Fe layer at the Fe–Cr interface ‘by hand’ (non-self-consistently; for spin-dependent reflection at Fe(001) see, e.g. Refs. [68–70]). Here, we point in particular to the experimental work of Fritzsche and coworkers on Fe/Cr multilayers [49,50] who found Cr moments perpendicular to the Fe magnetization. Such a magnetic configuration resulted in photoemission intensities (not shown here) that failed to agree with those of Dedkov [1].

### 3.3. Transition-matrix element effects

To briefly investigate matrix-element effects, the photoemission intensity is compared to spectral densities for the exemplary case of 4 ML Cr/Fe(110). For this purpose, the latter are computed

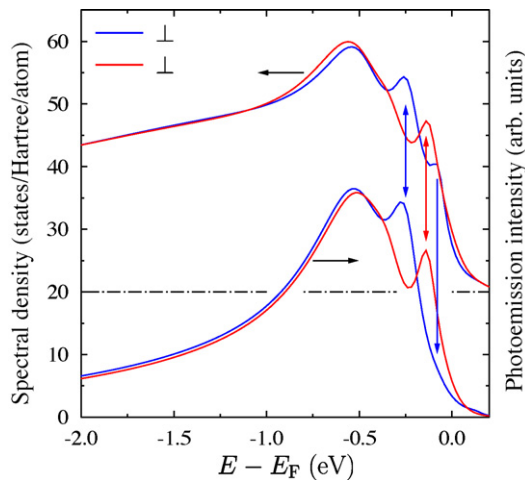


**Fig. 5.** Spin-resolved spectral density (top) and photoemission intensity (bottom) from 4 ML Cr/Fe(110), with spin-up (spin-down) data in blue (red). The spectral density of the subsurface Cr layer is offset by 20 states/Hartree/atom, with the associated ordinate on the left. The dashed-dotted line indicates the spectral-density zero. Vertical arrows mark spin-resolved quantum-well states which are discussed in the text. (For interpretation of the references to color in this figure legend, the reader is referred to the web version of the article.)

with the same energy-dependent self-energy as used for the photoemission spectra. Since the spectral density at small energies, in particular less than about  $-0.6$  eV, is smeared out, prominent maxima are observed in the energy range close to the Fermi energy  $E_F$  only (Fig. 5). These peaks originate from quantum-well states (QWS). Note that the spin polarization of these states alternate with energy. Further, the two states marked by double-pointed arrows show up clearly in the associated photoemission intensities, at  $-0.25$  eV (spin-up) and  $-0.14$  eV (spin-down). The spin-up maximum at  $-0.08$  eV, however, does not appear in the intensities (cf. the single-pointed arrow), which is attributed to dipole selection rules. A closer analysis reveals that a spin-up maximum is indeed present in the (partial) spectrum for s-polarized light, while for p-polarized light there is no maximum. Since the intensity for p-polarized light exceeds that for s-polarized light by about a factor of 30, the s-polarization maximum is covered by the p-polarization intensity.

The above analysis corroborates that a correct interpretation of experimental spectra has to consider matrix elements. In particular, it is hardly possible to conclude reliably from the photoelectron spin polarization on the initial-state spin polarization.

#### 4. Concluding remarks

Our *ab initio* study on the spin-resolved photoemission from Cr on Fe(110) reproduces major trends which have been found in Dedkov's experiment [1] but lack agreement in details. Our analysis suggests that the detailed magnetic structure at the Fe–Cr interface which essentially determines the spin-resolved photoemission intensities requires further experimental and theoretical investigations. Here, we would like to mention spin-resolved scanning tunneling microscopy [71] to reveal the magnetic structure of Cr films a very few ML thick. By this means, a possible noncollinear magnetic configuration may be deduced (see, e.g. Refs. [13,72]).

#### Acknowledgement

We acknowledge helpful discussions with Yu. S. Dedkov (Fritz-Haber-Institut, Berlin).

#### References

- [1] Y.S. Dedkov, Eur. Phys. J. B 57 (2007) 15.
- [2] F. Offi, W. Kuch, L.I. Chelaru, M. Kotsugi, J. Kirschner, J. Magn. Magn. Mater. 261 (2003) L1.
- [3] V. Skumryev, S. Stoyanov, Y. Zhang, G. Hadjipanayis, D. Givord, J. Nogués, Nature 423 (2003) 850.
- [4] M. Ali, C.H. Marrows, B.J. Hickey, Phys. Rev. B 67 (2003) 172405.
- [5] W. Kuch, L.I. Chelaru, F. Offi, J. Wang, M. Kotsugi, J. Kirschner, Nat. Mater. 5 (2006) 128.
- [6] J.S. Parker, L. Wang, K.A. Steiner, P.A. Crowell, C. Leighton, Phys. Rev. Lett. 97 (2006) 227206.
- [7] S.J. Lee, J.P. Goff, G.J. McIntyre, R.C.C. Ward, S. Langridge, T. Charlton, R. Dalgliesh, D. Mannix, Phys. Rev. Lett. 99 (2007) 037204.
- [8] U. Schlickum, N. Janke-Gilman, W. Wulfhekkel, J. Kirschner, Phys. Rev. Lett. 92 (2004) 107203.
- [9] L.M. Sandratskii, Adv. Phys. 47 (1998) 91.
- [10] G. Gubbiotti, G. Carlotti, M.G. Pini, P. Ploiti, A. Rettori, P. Vavassori, M. Ciria, R.C. O'Handley, Phys. Rev. B 65 (2002) 214420.
- [11] W. Kuch, L.I. Chelaru, F. Offi, J. Wang, M. Kotsugi, J. Kirschner, Phys. Rev. Lett. 92 (2004) 017201.
- [12] E. Martnez, A. Vega, R. Robles, A.L. Vázquez des Parga, Phys. Lett. A 337 (2005) 469.
- [13] S. Lounis, M. Reif, P. Mavropoulos, L. Glaser, P.H. Dederichs, M. Martins, S. Blügel, W. Wurth, Europhys. Lett. 81 (2008) 47004.
- [14] P. Bose, I. Mertig, J. Henk, Phys. Rev. B 75 (2007) 100402(R).
- [15] P. Bose, P. Zahn, I. Mertig, J. Henk, Phys. Rev. B 82 (2010) 014412.
- [16] R.S. Fishman, J. Phys.: Condens. Matter. 13 (2001) R235.
- [17] H. Zabel, J. Phys.: Condens. Matter. 11 (1999) 9303.
- [18] F.U. Hillebrecht, C. Roth, R. Jungblut, E. Kisker, A. Bringer, Europhys. Lett. 19 (1992) 711.
- [19] P. Fuchs, V. Petrov, K. Totland, M. Landolt, Phys. Rev. B 54 (1996) 9304.
- [20] A. Davies, J.A. Strosio, D.T. Pierce, R.J. Celotta, Phys. Rev. Lett. 76 (1996) 4175.
- [21] G. Panaccione, F. Sirotti, E. Narducci, G. Rossi, Phys. Rev. B 55 (1997) 389.
- [22] M. Freyss, D. Stoeffler, H. Dreyssé, Phys. Rev. B 56 (1997) 6047.
- [23] E.E. Fullerton, S.D. Bader, J.L. Robertson, Physics B 237–238 (1997) 234.
- [24] B. Heinrich, J.F. Cochran, T. Monchesky, R. Urban, Phys. Rev. B 59 (1999) 14520.
- [25] S. Heinze, P. Kurz, D. Wortmann, G. Bihlmayer, S. Blügel, Appl. Phys. A 75 (2002) 25.
- [26] M. Bode, R. Wiesendanger, in: H. Hopster, H.P. Oepen (Eds.), Magnetic Microscopy of Nanostructures, Springer, Berlin, 2005, p. 203.
- [27] W. Wulfhekkel, J. Kirschner, Annu. Rev. Mater. Res. 37 (2007) 69.
- [28] M.A. van Hove, S.Y. Tong, Surface Crystallography by LEED. Theory, Computation and Structural Results, Vol. 2: Springer Series in Chemical Physics, Springer, Berlin, 1979.
- [29] R. Feder, J. Phys. C: Sol. State Phys. 14 (1981) 2049.
- [30] T. Greber, Baberschke et al. [55], Vol. 580: Lecture Notes in Physics, p. 94.
- [31] W. Schattke, M.A. van Hove (Eds.), Solid-State Photoemission and Related Methods. Theory and Experiment, Wiley-VCH, Weinheim, 2003.
- [32] J. Osterwalder, Lect. Notes Phys. 697 (2006) 95.
- [33] F. Schiller, D.V. Vyalikh, V.D.P. Servidio, S.L. Molodtsov, Phys. Rev. B 70 (2004) 174444.
- [34] J. Meersschaut, J. Dekoster, S. Demuyck, S. Cottenier, B. Swinnen, M. Rots, Phys. Rev. Lett. 57 (1998) R5575.
- [35] M.P. Seah, W.A. Dench, Surf. Interface Anal. 1 (1979) 2.
- [36] H.-J. Drouhin, Phys. Rev. B 56 (1997) 14886.
- [37] H. Hopster, J. Electron. Spectrosc. Relat. Phenom. 98–99 (1999) 15.
- [38] A. Ernst, J. Henk, R.K. Thapa, J. Phys.: Condens. Matter. 17 (2005) 3269.
- [39] U. Schlickum, C.L. Gao, W. Wulfhekkel, J. Henk, P. Bruno, J. Kirschner, Phys. Rev. B 74 (2006) 054409.
- [40] D.F. Johnson, D.E. Jiang, E.A. Carter, Surf. Sci. 601 (2007) 699.
- [41] D.V. Vyalikh, P. Zahn, M. Richter, Y.S. Dedkov, S.L. Molodtsov, Phys. Rev. B 72 (2005) 041402(R).
- [42] J. Henk, B. Johansson, J. Electron. Spectrosc. Relat. Phenom. 105 (1999) 187.
- [43] J. Henk, M. Hoesch, J. Osterwalder, A. Ernst, P. Bruno, J. Phys.: Condens. Matter. 16 (2004) 7581.
- [44] M. Mulazzi, M. Hochstrasser, M. Corso, I. Vobornik, J. Fujii, J. Osterwalder, J. Henk, G. Rossi, Phys. Rev. B 74 (2006) 035118.
- [45] S.H. Vosko, L. Wilk, M. Nusair, Can. J. Phys. 58 (1980) 1200.
- [46] I. Mertig, E. Mrosan, P. Ziesche, Multiple Scattering Theory of Point Defects in Metals: Electronic Properties, B.G. Teubner, Leipzig, 1987.
- [47] A. Gonis, Green Functions for Ordered and Disordered Systems, Vol. 4: Studies in Mathematical Physics, North-Holland, Amsterdam, 1992.
- [48] J. Zabloudil, R. Hammerling, L. Szunyogh, P. Weinberger (Eds.), Electron Scattering in Solid Matter, Springer, Berlin, 2005.
- [49] H. Fritzsche, J. Hauschild, A. Hoser, S. Bonn, J. Klenke, Europhys. Lett. 49 (2000) 507.
- [50] H. Fritzsche, S. Bonn, J. Hauschild, J. Klenke, K. Prokes, G.J. McIntyre, Phys. Rev. B 65 (2002) 144408.
- [51] M. Johnson, P. Bloemen, J. de Vries, Rep. Prog. Phys. 59 (1996) 1409.
- [52] K. Baberschke, Baberschke et al. [55], Vol. 580: Lecture Notes in Physics, p. 27.
- [53] K.D. Usadel, F. Hucht, Phys. Rev. B 66 (2002) 024419.
- [54] D. Sander, J. Phys.: Condens. Matter. 16 (2004) R603.
- [55] K. Baberschke, W. Nolting, M. Donath (Eds.), Band-Ferromagnetism: Ground-State and Finite-Temperature Phenomena, Vol. 580: Lecture Notes in Physics, Springer, Berlin, 2001.

- [56] H.D. Shih, F. Jona, U. Bardi, P.M. Marcus, *J. Phys. C: Sol. State Phys.* 13 (1980) 3801.
- [57] J. Braun, *Rep. Prog. Phys.* 59 (1996) 1267.
- [58] J. Henk, H. Mirhosseini, P. Bose, K. Saha, N. Fomynikh, T. Scheunemann, S.V. Halilov, E. Tamura, R. Feder, *OMNI—Fully Relativistic Electron Spectroscopy Calculations*, 2009.
- [59] J. Henk, in: H.S. Nalwa (Ed.), *Handbook of Thin Film Materials*, vol. 2, Academic Press, San Diego, 2001, p. 479, Ch. 10.
- [60] A. Rampe, G. Güntherodt, D. Hartmann, J. Henk, T. Scheunemann, R. Feder, *Phys. Rev. B* 57 (1998) 14370.
- [61] I.H. Inoue, I. Hase, Y. Aiura, A. Fujimori, Y. Haruyama, T. Maruyama, Y. Nishishira, *Phys. Rev. Lett.* 74 (1995) 2539.
- [62] J. Henk, T. Scheunemann, S.V. Halilov, R. Feder, *J. Phys.: Condens. Matter* 8 (1996) 47.
- [63] A. Rampe, D. Hartmann, G. Güntherodt, in: H. Ebert, G. Schütz (Eds.), *Spin–Orbit Influenced Spectroscopies of Magnetic Solids*, No. 466 in *Lecture Notes in Physics*, Springer, Berlin, 1996, p. 49.
- [64] Y.S. Dedkov, *Eur. Phys. J. B* 47 (2005) 315.
- [65] E. Tamura, R. Feder, G. Waller, U. Gradmann, *Phys. Stat. Sol. (b)* 157 (1990) 627.
- [66] S. Ohnishi, A.J. Freeman, M. Weinert, *Phys. Rev. B* 28 (1983) 6741.
- [67] R. Feder, J. Henk, in: H. Ebert, G. Schütz (Eds.), *Spin–Orbit Influenced Spectroscopies of Magnetic Solids*, No. 466 in *Lecture Notes in Physics*, Springer, Berlin, 1996, p. 85.
- [68] S. De Rossi, A. Tagliferri, F. Ciccacci, *J. Magn. Magn. Mater.* 157/158 (1996) 287.
- [69] C.M. Wei, M.Y. Chou, *Phys. Rev. B* 68 (2003) 125406.
- [70] J.J. Paggel, T. Miller, T.-C. Chiang, *J. Electron. Spectrosc. Relat. Phenom.* 101–103 (1999) 271.
- [71] R. Wiesendanger, *Rev. Mod. Phys.* 81 (4) (2009) 1495, <http://link.aps.org/abstract/RMP/v81/p1495>.
- [72] C.L. Gao, A. Ernst, A. Winkelmann, J. Henk, W. Wulfhekkel, J. Kirschner, *Phys. Rev. Lett.* 100 (2008) 237203.